Supporting information for:

Structural basis for complement Factor I control and its disease-associated sequence polymorphisms.

Pietro Roversi[1a], Steven Johnson[1a], Joseph J.E. Caesar[a], Florence McLean[a], Kirstin J. Leath[a], Stefanos A. Tsiftsoglou[b], B. Paul Morgan[c], Claire L. Harris[c], Robert B. Sim[b] and Susan M. Lea[a23]

[a]: Sir William Dunn School of Pathology, University of Oxford, South Parks Road, Oxford OX1 3RE, England, UK;

[b]: Department of Biochemistry, University of Oxford, South Parks Road, Oxford OX1 3QU, England, UK;

[c]: Department of Infection, Immunity and Biochemistry, School of Medicine, Cardiff University, Heath Park, Cardiff CF14 4XN, Wales, UK

The authors declare no conflict of interest.

Classification: Biological Sciences, Biochemistry[4]

---

[1] P.R. and S.J. contributed equally to this work

[2] To whom correspondence may be addressed. E-mail: susan.lea@path.ox.ac.uk, tel.: 0044-1865-275181; fax: 0044-1865-275556

[3] Author contributions: P.R., S.J., R.B.S., B.P.M, C.L.H. and S.M.L. designed research; P.R., S.J., J.J.E.C., F.M., K.J.L, S.A.T. and S.M.L. performed research; P.R., S.J., J.J.E.C., F.M., K.J.L, B.P.M, C.L.H., S.A.T. and S.M.L.analyzed data; and P.R., S.J. and S.M.L. wrote the paper.

[4] The coordinates and measured structure factor amplitudes for the Factor I crystal have been deposited in the Protein Data Bank (accession code 2XRB).

Fig S1. Factor I sequence alignment across species.

The fI sequences belong to the following database entries: Man (*Homo sapiens*) GI:1335054; Orangutan (*Pongo abelii*) GI:197098986; Rabbit (*Oryctolagus cuniculus*) GI:291401284; Rat (*Rattus norvegicus*) GI:13162353; Mouse (Mus musculus) GI:110347406; Panda (*Ailuropoda melanoleuca*) GI:281338891; Dog (*Canis familiaris*) GI:74002138; Horse (*Equus caballus*), GI:194208523; Cow (*Bos Taurus*) GI:84000165; Frog (*Xenopus tropicalis*) GI: 73853846|; Chicken (*Gallus gallus*) GI:118090385; Shark (*Triakis scyllium*) GI:21669679; Lamprey (*Lethenteron japonicum*) GI:194686864.

Red boxes with white lettering: 100% conserved residues; white boxes and red lettering: residues with high level of similarity across the sequences. The figure was prepared with the ClustalW alignment program and the ESPript server (http://espript.ibcp.fr/ESPript/ESPript/).

Fig. S2. Representative electron density of glycosylation

The 1 sigma level contour of the 2Fo-Fc electron density map is represented as a mesh around the region of the serine protease domain containing the N-linked glycosylation at Asn 446 (copy B). Only the first GlcNAc residue was traced at all 4x6 glycosylation sites, although some electron density for the second GlcNAc residue of the glycan was visible in places.

Fig. S3. Structure-annotated sequence

The sequence of human fI is annotated with the secondary structure as observed in the crystal, coloured as in the cartoon schematic. Boxed residues are highly mobile and could not be traced in some or all the copies of the molecule in the asymmetric unit of the crystal. Disulphide bonds are represented as lines between Cys residues, the cysteines of the interchain disulphide bond are additionally flagged with triangles. The six glycosylated Asn residues are starred. The residues coordinating the Ca atoms are flagged with purple circles. The catalytic triad residues His362, Asp411 and Ser507 are highlighted by red boxes.

Fig. S4 The individual domains of fI.

A: Schematic representation of the structure of fI. Blue: FIMAC domain; green: SRCR domain; orange and yellow: LDLRA1 and LDLRA2 domains; the N- and C-termini of the heavy chain and the loops between its 4 domains are in black; the region connecting the FIMAC and the SRCR domains and the one between the LDLRA2 and the Cterminus of the heavy chain were missing in the crystal electron density and are dashed. Red: serine protease domain. White stars flag the N-linked glycosylation sites. **B,C,D,E:** individual domains, in cartoon and surface representation, with disulphide bonds in ball-and stick, and the N-linked GlnNAcs in ball-and-stick, painted cyan. **B.** Factor I Membrane Attack Complex (FIMAC) domain; **C.** Scavenger Receptor Cystein Rich (SRCR) domain. **D.** Low-Density Lipoprotein Receptor type A (LDLRA) domains 1 and 2; each domain binds a Calcium ion represented as a purple sphere; **E.** Serine protease (SP) domain.

Fig. S5 Closest structural homologues of the fI domains

Structural homologues of each domain were identified using the Dali server (1). (**A**) The FIMAC domain overlayed on the follistatin-domain of BM-40 (rmsd = 2.5Å over 65 Cα atoms). This fold is also found in the FIMAC domains of complement component C7. Intriguingly, the next closest structural homologues are ovomucoid serine protease inhibitors as earlier proposed on the basis of sequence (1). However, the location of the FIMAC and the extensive covalent and non-covalent interactions locking it in place within the heavy chain demonstrate that it cannot be acting in this fashion as previously proposed on the basis of small angle X-ray scattering studies (2). In addition, despite a high level of structural similarity in the loop equivalent to the ovomucoid inhibitory region, the glycosylation of Asn52 of fI would prevent docking of this region into a protease active site and so excludes the possibility of the fI FIMAC acting to inhibit another circulating protease. The structural homology to this inhibitor class therefore seems irrelevant to the function of the fI FIMAC as previously suggested (2). (**B**) The SRCR domain overlayed on the SRCR domain of Mac-2 binding protein (rmsd = 2.5Å over 96 Cα atoms). The SRCR domain is also related to the SRCR domain of hepsin, another mosaic serine protease. Unlike hepsin, however, the SRCR domain of fI does not form any contacts with the serine protease domain. (**C**) LDLRA1 domain overlayed on the first LDLR domain of Apolipoprotein E receptor 2 (rmsd = 0.6Å over 30 Cα atoms). (**D**) LDLRA2 domain overlayed on ligand binding repeat 5 of the low-density lipoprotein receptor (rmsd = 1.0Å over 37 Cα atoms). (**E**) SP domain overlayed on Hepatocyte growth factor activator (rmsd = 1.7Å over 180 Cα atoms).
Blue: fI domains; pink: structurally homologous domains obtained by searching with the individual fI domains against the protein databank using the DALI server (3). Disulphide bonds are represented in sticks, the Ca^{++} ions as spheres.

Fig. S6 Thrombin zymogen site, exosites and allostery in SP domains.

Thrombin (from PDB ID 1P8V) is in surface representation, with the zymogen activation domain coloured blue, and the sites of allosteric control (Exosites I and II) coloured red. The structure of fI was aligned with the one of thrombin, by superposing the serine protease domains, and the heavy chain of the fI model aligned on thrombin is represented in green cartoon.

Fig. S7 Modeling fI binding on the C3b substrate loop

(**A**) Overlay of the ^{1279}PSRSSK^{1284} region of C3b in purple ball-and-stick, with the pseudo-substrate peptide ^{37}LCKARF^{42} from the TdPI inhibitor protein, green ball-and-stick (C3b: PDB ID 2WII; trypsin:TdPI: 2UUY); (**B**) fI (grey) is oriented by superposition of its serine protease domain onto the trypsin domain in the trypsin (purple): TdPI (green) complex.

Fig. S8 The glycosylation on factor I cluster on one side of the molecule and do not impede fH and C3b binding in the model for the ternary complex.

Factor I is shown in black cartoon, with the glycosylated Asn residues in sticks, and a model for the N-linked $Man_3GlcNAc_2$ core structure in spheres, colored by atom type (C, green; O, red; N, blue). The binary complex C3b:fH in surface representation, coloured as in Fig. 6 of the main paper. The glycans were modelled using the GlyProt server at http://www.glycosciences.de/modeling/glyprot.

Fig. S9 Electrostatic potential surfaces for fI and the FH_{1-4}/C3b complex.

Left hand side: the C3b:fH_{1-4} complex from PDB ID 2WII is represented as a surface, coloured by the electrostatic potential: red: -3.0 kT/e, blue: +3.0 kT/e with the fI footprint on the complex outlined in black. Right hand side: the surface of factor I, coloured by its electrostatic potential at the same contour levels as the C3b:fH_{1-4} complex and oriented by opening up the ternary complex with a rotation of fI by 180° along the vertical direction. Positively charged regions at the edges of that face of fI sit opposite negatively charged patches on C3b:fH_{1-4}.

Fig. S10 ^{125}I-C3(NH_3) proteolysis by redissolved fI protein crystals.

Proteolytic activity of human fI from crystals grown in 30% PEG600, imidazole malate 10 mM pH 4.5. Crystals were re-dissolved in 10 mM K_3PO_4 pH 6.2, 0.5 mM EDTA, 0.1% TWEEN-20. Reaction mixtures contained 0.4 nM ^{125}I-C3(NH_3), 4 nM fH and 4.5 nM of fI from re-dissolved crystals or serum-purified controls. Reactions were quenched by addition of SDS-PAGE sample buffer with 20 mM DTT.

Table S1. Data collection and refinement statistics

Table S2. Proposed explanation for disease-associated polymorphisms and mutants of factor I described in the literature.

Factor I mutants and polymorphisms reported in the literature as associated with disease are listed with the appropriate references, and grouped in the table according to the rational for their effect, as inferred on the basis of the fI crystal structure.

Movie S1. Assembly of the ternary complex.

The movie illustrates the cofactor approaching the C3b molecule and forming the interaction surface for fI. Once fI docks onto it, the first cleavage occurs.

Fig. S1. Factor I sequence alignment across species.

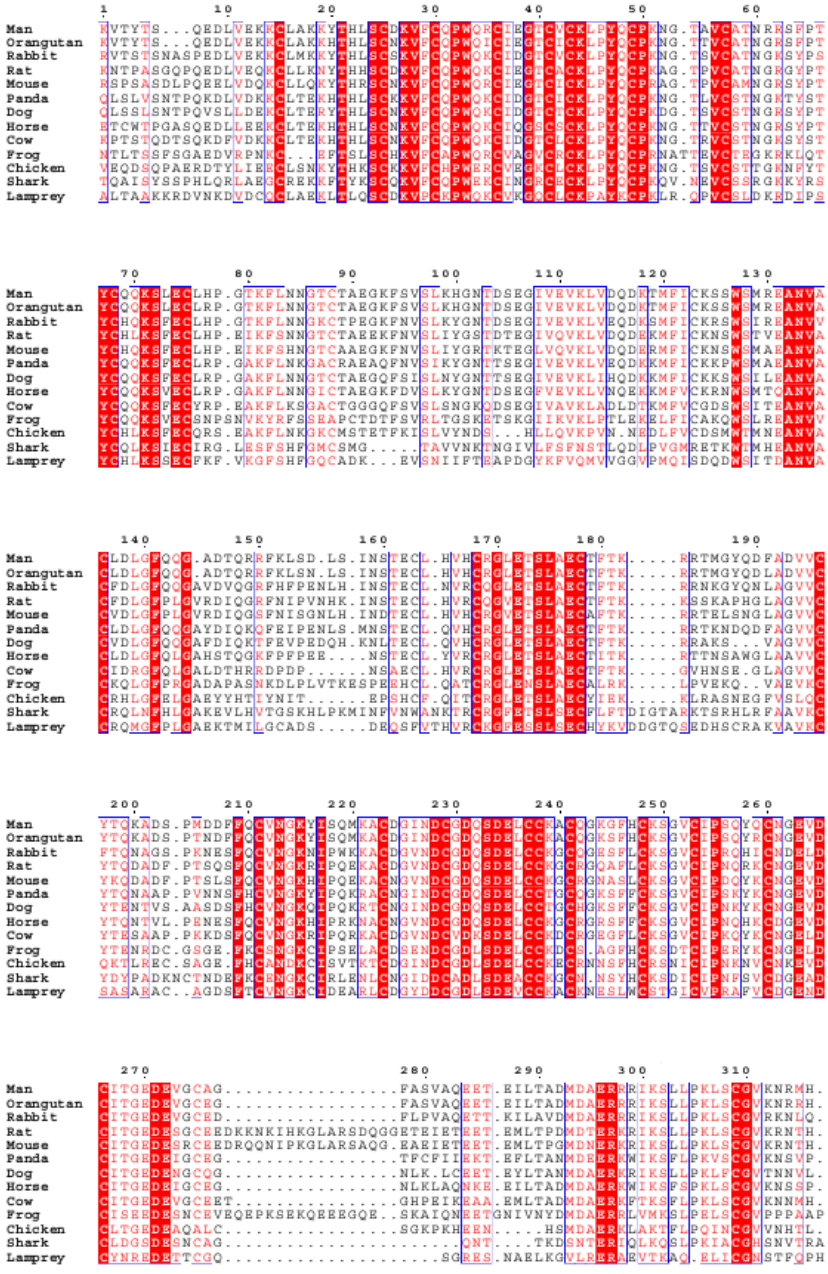

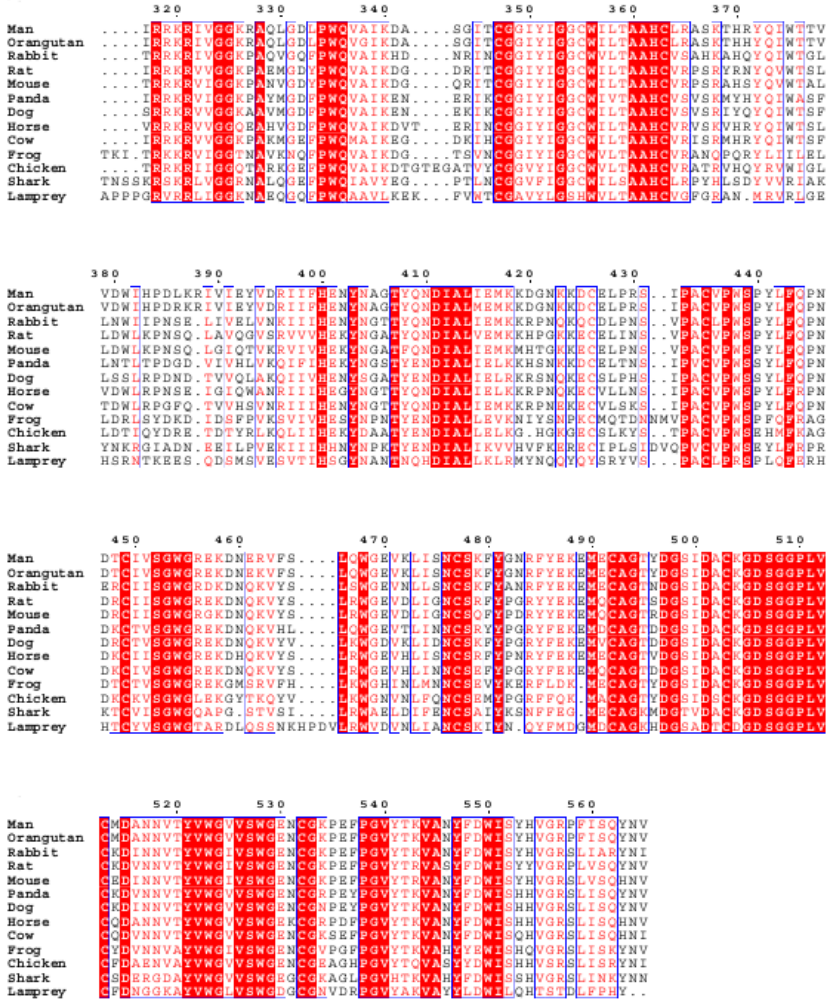
320 330 340 350 360 370
Man ....IRRKRIVGGKEAQLGDLPWQVAIKDA....SGITCGGIYIGGCWILTAAHCLKASKTHRYQIWTTV
Orangutan ....IRRKRIVGGKEAQLGDLPWQVGIKDA....SGITCGGIYIGGCWILTAAHCLKASKTHHYQIWTTV
Rabbit ....TRRKRIVGGKEAQVGQFPWQVAIKHD....NRINCGGIYIGGCWVLTAAHCVSAHKAHQYQIWTGL
Rat ....IRRKRVVGGKEAEMGDYPWQVAIKDG....DRITCGGIYIGGCWILTAAHCVKPSRYRNYQVWTSL
Mouse ....TRRKRVIGGKEANVGDYPWQVAIKDG....QRITCGGIYIGGCWILTAAHCVKPSRAHSYQVWTAL
Panda ....IRRKRVIGGKEAYMGDFPWQVAIKEN....ERIKCGGIYIGGCWIVTAAHCVSVSKMYHYQIWASF
Dog ....SRRKRVVGGKEAVMGDFPWQVAIKEN....EKIKCGGIYIGGCWILTAAHCVSVSRIYQYQIWTSF
Horse ....VRRKRVVGGQEAHVGDFPWQVAIKDVT...ERINCGGIYIGGCWILTAAHCVRVSKVHRYQIWTSL
Cow ....IRRKRVVGGKEAKMGEFPWQMAIKEG....DKIHCGGIYIGGCWILTAAHCVRISRMHRYQIWTSF
Frog TKI.TRKKRVIGGTNAVKNQFPWQVAIKDG....TSVNCGGIYIGGCWVLTAAHCVRANQPQRYLIILEL
Chicken ....TRRKRIGGQTAKKGEFPWQVAIKDTGTEGATVYCGGVYIGGCWVLTAAHCVRATRVHQYRVWIGL
Shark TNSSKRSKRLVGGRNALQGEFPWQIAVYEG....PTLNCGGVFIGGCWILSAAHCLRPYHLSDYVVRIAK
Lamprey APPPGRVRRLIGGKNAEQGQFPWQAAVLKEK...FVVMTCGAVYLGSHWVLTAAHCVGFGEAN.MRVRLGE
380 390 400 410 420 430 440
Man VDWIHPDLKRIVIEYVDRIIFHENYNAGTYQNDIALIEMKKDGNKKDCELPRSIIPACVPWSPYLFQPN
Orangutan VDWIHPDRKRIVIEYVDRIIFHENYNAGTYQNDIALMEMKKDGNKKDCELPRSIIPACVPWSPYLFQPN
Rabbit LNWIIPNSE.LIVELVNKIIIHENYNGTTYQNDIALIEMKKRPNQKQCDLPNSVVPACLPWSPYLFQPN
Rat LDWLKPNSQ.LAVQGVSRVVVHEKYNGATYQNDIALVEMKKHPGKKECELINSVVPACVPWSPYLFQPN
Mouse LDWLKPNSQ.LGIQTVKRVIVHEKYNGATYQNDIALIEMKMHTGKKECELPNSVVPACVPWSPYLFQPN
Panda LNTLTPDGD.VIVHLVKQIPIHEKYNGSTYENDIALIELKKHSNKKDCELTNSIIPACVPWSSYLFQPN
Dog LSSLRPDND.TVVQLAKQIVIHENYSGATYENDIALIELRKRSNQKECSLPHSIIPACVPWSSYLFQPN
Horse VDWLRPNSE.IGIQWANRIIIHEGYNGTTYQNDIALIELKKRPNQKECVLLNSIIPACVPWSPYLFRPN
Cow TDWLRPGFQ.TVVHSVNRIIIHENYNGTTYQNDIALIEMKKRPNEKECVLSKSIIPACVPWSPYLFQPN
Frog LDRLSYDKD.IDSFPVKSVIVHESYNPNTYENDIALLEVKNIYSNEKCMQTDNNMVPACVPWSPFCFRAG
Chicken LDTTQYDRE.TDTYRLKQLIIHEKYDAATYENDIALLELKG.HGKKGECSLKYSITPACVPWSEHMFNAG
Shark YNKRGIADN.EEILPVEKIIIHENYNPKTYENDIALIKVVHVFKERECIPLSIDVQPACVPWSEYLFRPR
Lamprey HSRNTKEES.QDSMSVESVTIHSGYNANTYNQHDIALLKLRMYNQKYYQYSRYVSSIAPACLPRSPLQFERH
450 460 470 480 490 500 510
Man DTCIVSGWGREKDNERVFSLQWGEVKLISNCSKFYGNRFYEKEMECAGTYDGSIDACKGDSGGPLV
Orangutan DTCIVSGWGREKDNEKVFSLQWGEVKLISNCSKFYGNRFYEKEMECAGTYDGSIDACKGDSGGPLV
Rabbit ERCIISGWGRDKDNQKVYSLSWGEVNLLSNCSKFYANRFYEKEMECAGINDGSIDACKGDSGGPLV
Rat DRCIISGWGREKDNQKVYSLRWGEVDLIGNCSRFYPGRYYEKEMECAGTSDGSIDACKGDSGGPLV
Mouse DRCIISGWGRGKDNQKVYSLRWGEVDLIGNCSQFYPDRYYEKEMECAGTRDGSIDACKGDSGGPLV
Panda DKCIVSGWGREKDNQKVHLLQWGEVTLINNCSRYYPGRYFEKEMECAGTDDGSIDACKGDSGGPLV
Dog DRCIVSGWGREKDNQKVYVLKWGDVKLIDNCSKFYPGRYFEKEMECAGTDDGSIDACKGDSGGPLV
Horse DKCIISGWGREKDHQKVYSLRWGEVHLISNCSRFYPNRYFEKEMECAGTVDGSIDACKGDSGGPLV
Cow DKCIVSGWGREKDNQKVYSLRWGEVHLINNCSEFYPGRYFEKEMECAGTDDGSIDACKGDSGGPLV
Frog DTCIVSGWGREKGMSRVFHLKWGHINLMNNCSEYYKERFLDKMECAGTYDGSIDACKGDSGGPLV
Chicken DKCKVSGWGLEKGYTKQYVLKWGNVNLFQNCSEMYPGRFFQKMACAGTYDGSIDSCKGDSGGPLV
Shark KTCVISGWGQAPGLSTVSILRWAELDLPENCSAIYKSNFFEGMRCAGKMDGTVDACKGDSGGPLV
Lamprey HTCVVSGWGTARDLQSSNKHPDVLRWVDVNLIANCSKIYN.QYFMDGMRCAGFHDGSADTCKGDSGGPLV
520 530 540 550 560
Man CMDANNVTYVWGVVSWGENCGKPEFPGVYTKVANYFDWISYHVGRPFISQYNV
Orangutan CMDANNVTYVWGVVSWGENCGKPEFPGVYTKVANYFDWISYHVGRPFISQYNV
Rabbit CKDINNVTYVWGIVSWGENCGKPEFPGVYTRVANYFDWISYHVGRSLIARYNI
Rat CKDVNNVTYVWGIVSWGENCGKPEFPGVYTRVANYFDWISYYVGRPLVSQYNV
Mouse CKDINNVTYVWGIVSWGENCGKPEFPGVYTKVANYFDWISYHVGRSLVSQHNV
Panda CKDVNNVTYVWGVVSWGENCGRPEYPGVYTKVANYFDWISHHVGRSLISQYNV
Dog CKDINNVTYVWGVVSWGENCGNPEYPGVYTKVANYFDWISHHVGRSLISQYNV
Horse CQDANNVTYVWGVVSWGEHCGRPDPPGVYTKVANYFDWISHHVGRSLISQHNV
Cow CQDVNNVTYVWGVVSWGENCGKSEPPGVYTKVANYFDWISQHVGRSLISQHNI
Frog CYDVNNVAYVWGIVSWGENCGVPGPPGVYTKVAHYYEWISHQVGRSLISKYNV
Chicken CPDAENVAYVWGVVSWGENCGEAGHPGVYTQVASYYDWISHHVSRSLISRYNI
Shark CSDERGDAYVWGVVSWGEGCGKAGLPGVHTKVAHYFDWISSHVGRSLINKYNN
Lamprey CPDNGGKAYVWGLVSWGDGCGNVDRPGVYARVAYYLDWILQHTSTDLFPHY..

Fig. S2 Representative electron density of glycosylation

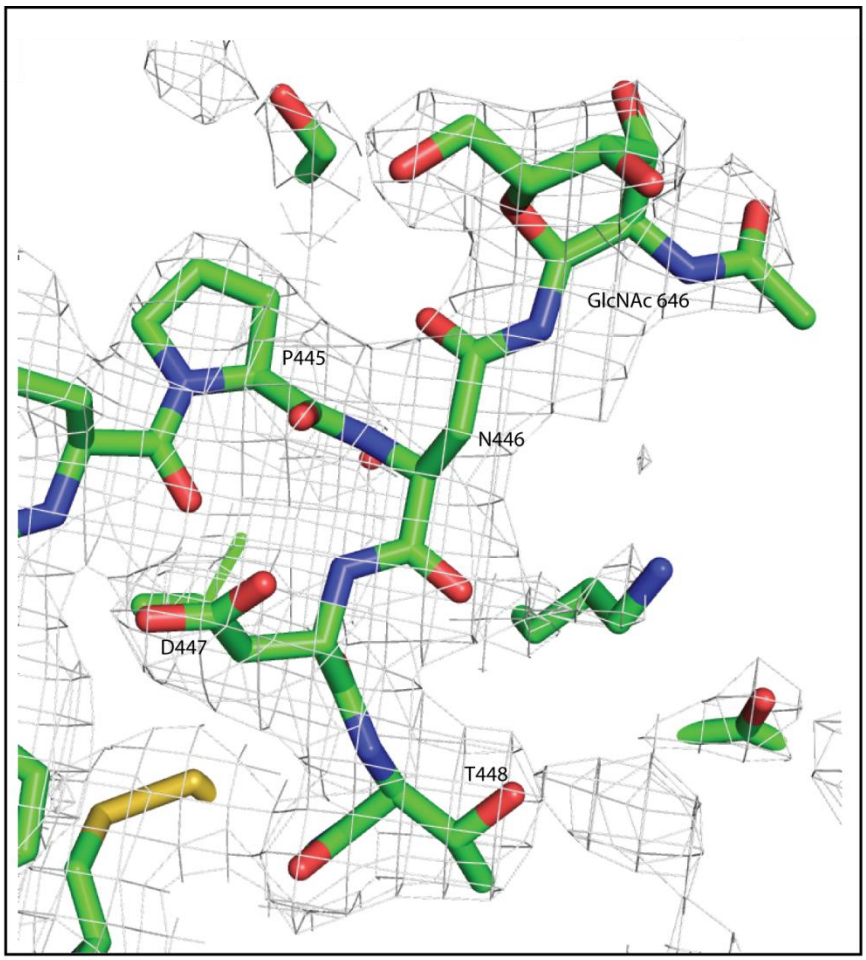

Fig. S3 Structure-annotated equence

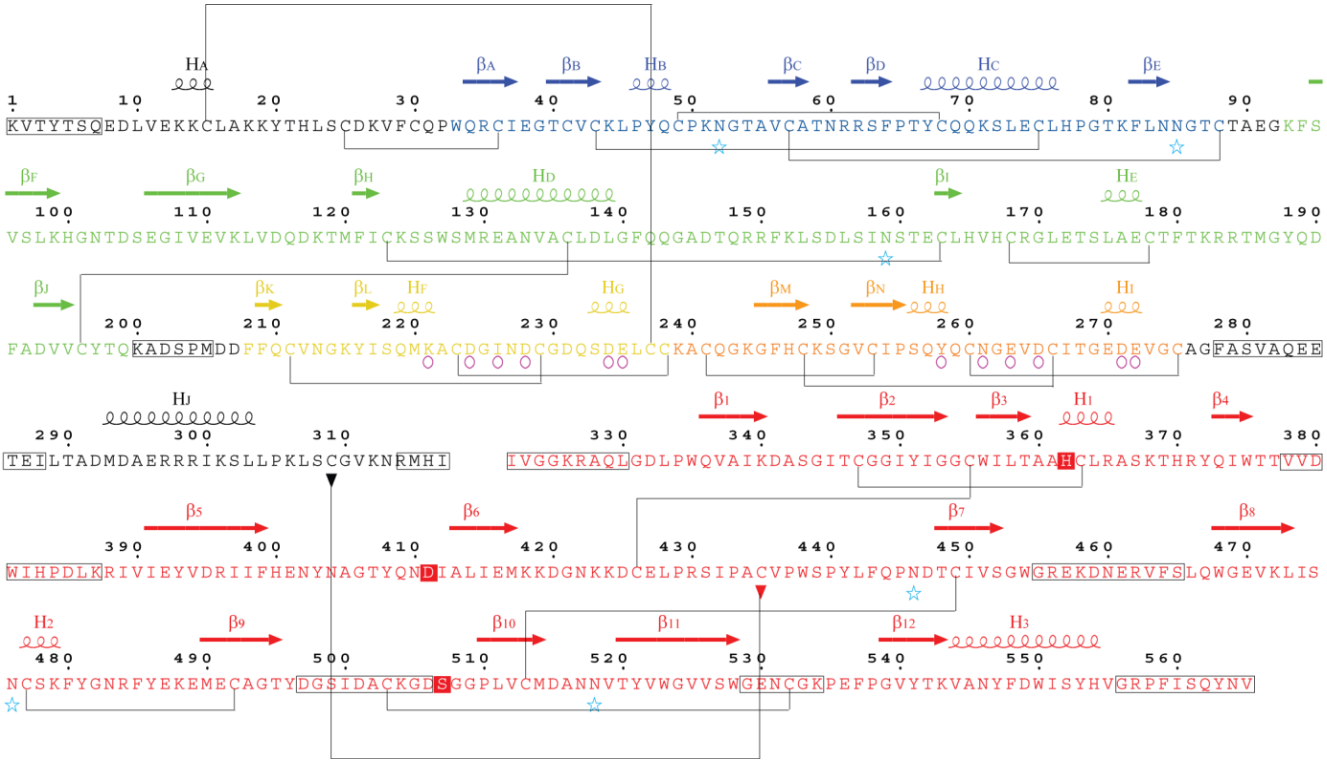

Fig. S4 The individual domains of fI.

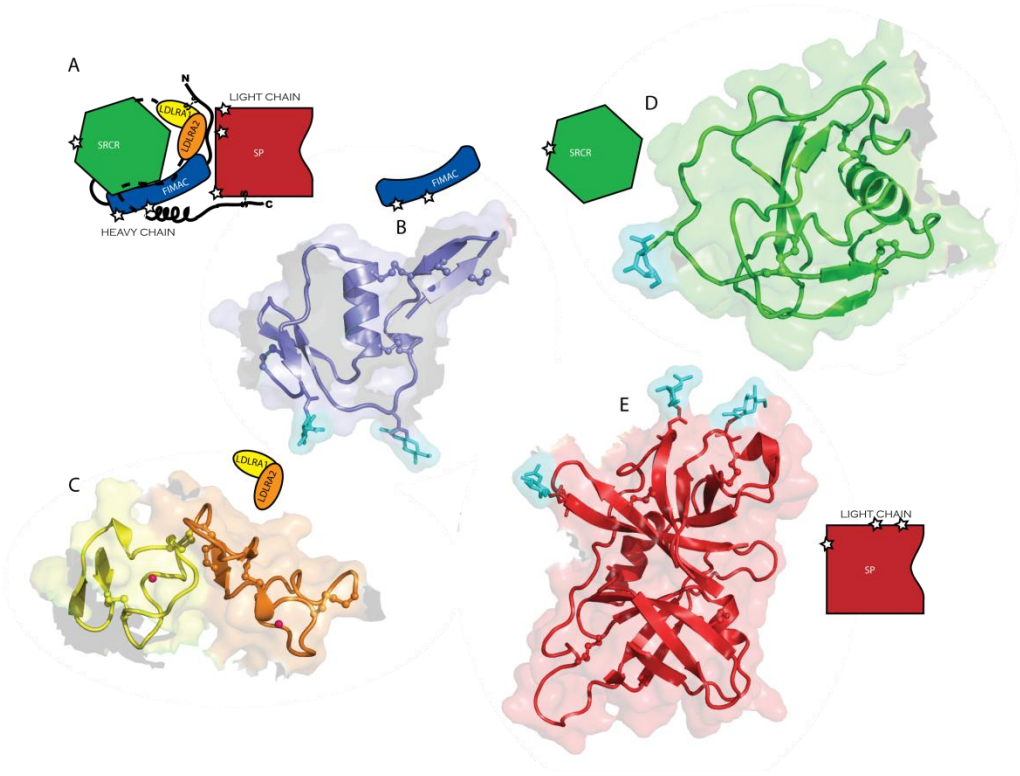

Fig. S5 Closest structural homologues of the fI domains and their rmsd Cα to fI domains

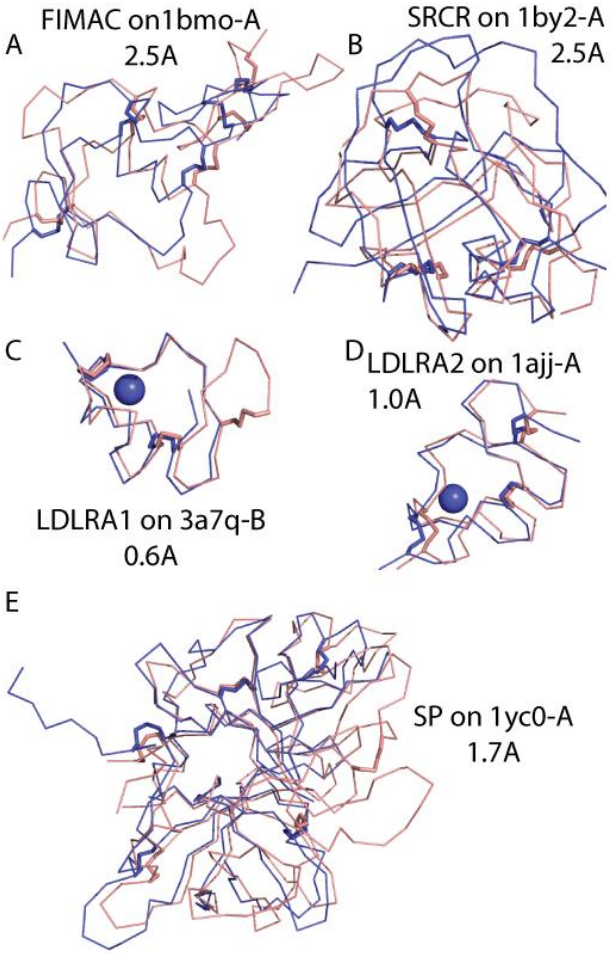

Fig. S6 Thrombin zymogen site, exosites and allostery in SP domains.

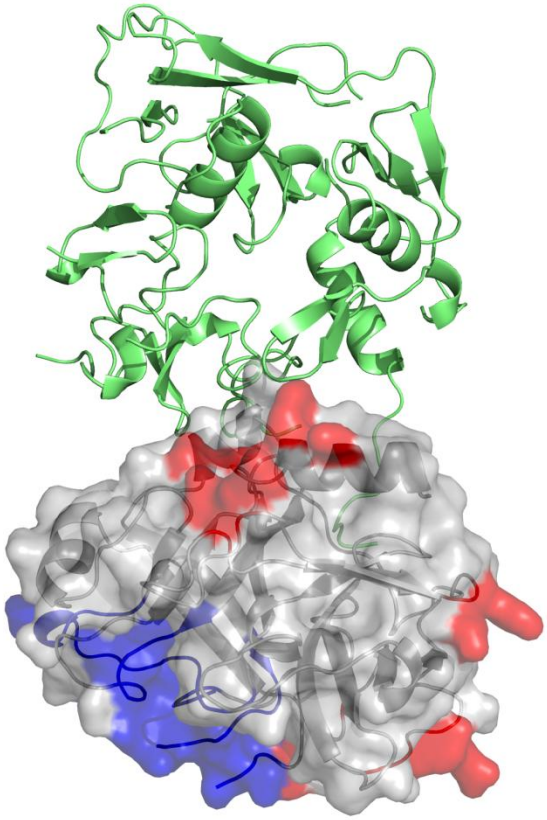

Fig. S7 Modeling of fI binding on the C3b substrate loop.

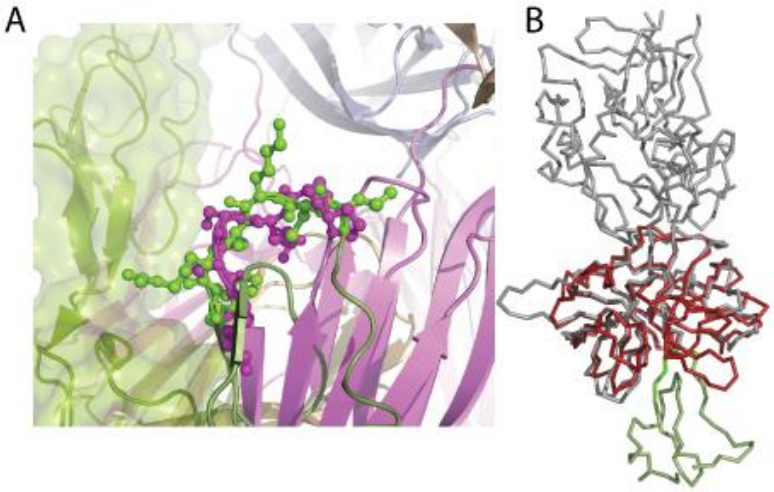

Fig. S8 The glycosylation on factor I cluster on one side of the molecule and do not impede fH and C3b binding in the model for the ternary complex.

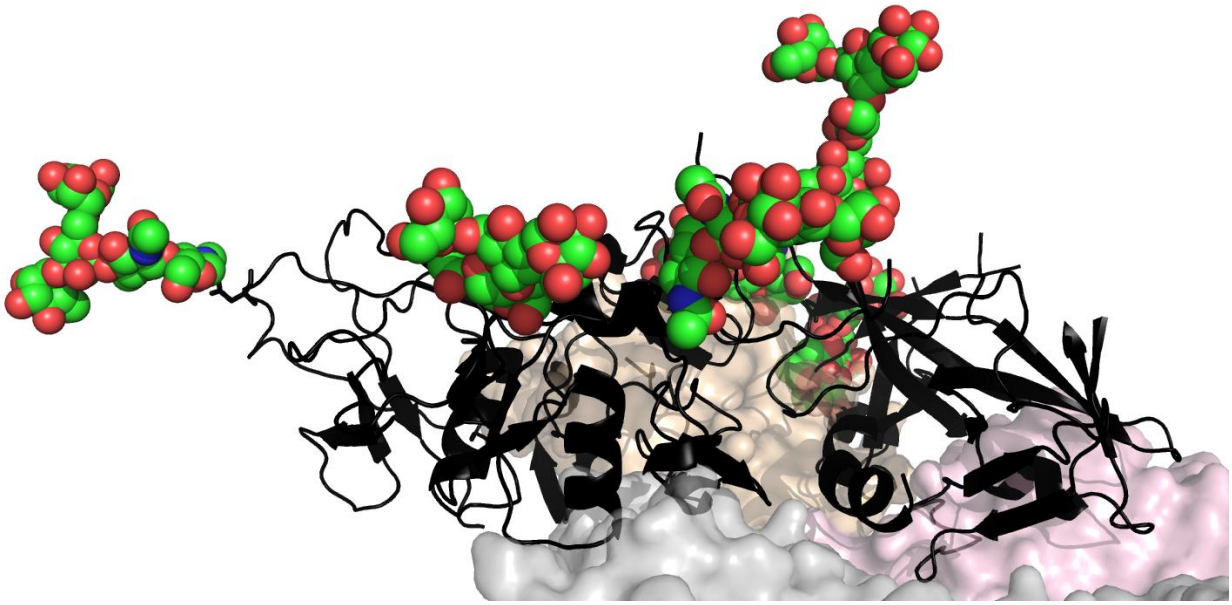

Fig. S9 Electrostatic potential surfaces for fI and the fH1-4/C3b complex.

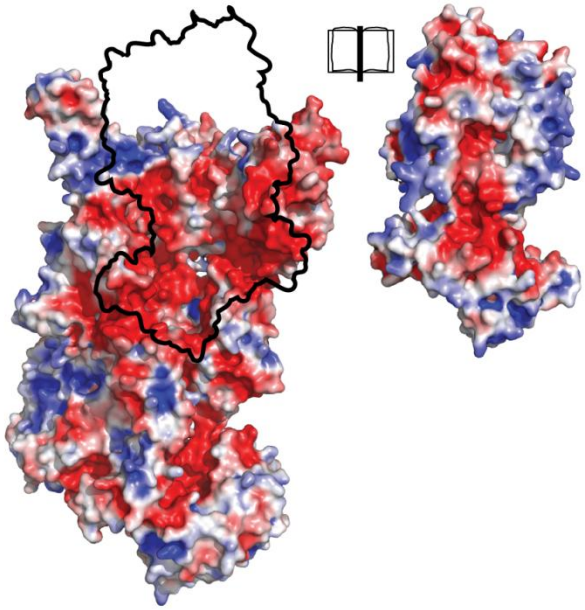

Fig. S10 ^{125}I-C3(NH_3) proteolysis by redissolved fI protein xtals.

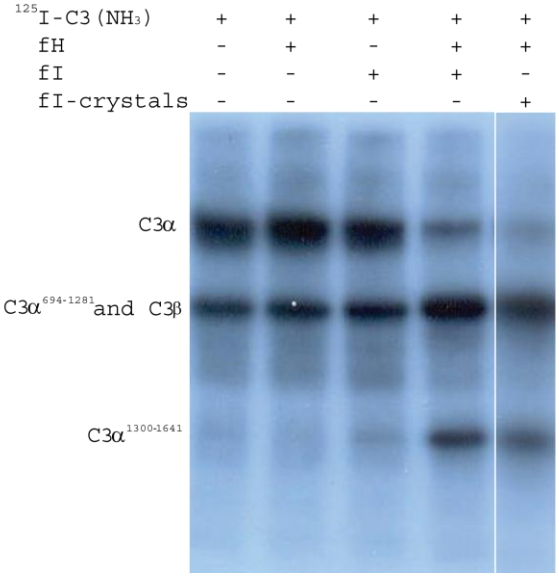

Table S1 Data collection and refinement statistics

	Human fI[†]
Space group	P1
Cell dimensions	
a, *b*, *c* (Å)	71.32, 234.72,40.30
α,β,γ (°)	89.98,90.18,90.03
Resolution (Å)	78.3-2.7
	(2.8-2.7)*
R_{sym} or R_{merge}	0.11(0.41)
$I / \sigma I$	10.5(2.0)
Completeness (%)	90.8(90.1)
Redundancy	2.9(2.5)
Refinement	
Resolution (Å)	79-2.69
No. reflections	61930
R_{work} / R_{free}	0.20 / 0.24
No. atoms	
Protein	14581
Ligand/ion	18 NAG (324 atoms)
	8 Ca^{+2} ions
Water	0
B-factors (Å^2)	
Protein	49.5
Ligand/ion	66.4
Water	-
R.m.s. deviations	
Bond lengths (Å)	0.006
Bond angles (°)	1.96

Values in parentheses are for highest-resolution shell.

*A single crystal was used for all data collections

†: tetartohedrally twinned; twin operator (twin fraction): hkl (0.33); -hk-l (0.36); -h-kl (0.21); h-k-l (0.10)

Table S2 Proposed explanation for disease-associated polymorphisms and mutants of factor I described in the literature.

Disrupt structure				Disrupt interactions with substrate or cofactor
Affect catalytic site	Disrupt domain fold	Disrupt interdomain packing		
		Within the heavy chain	Between heavy- and light-chain	
I322T, D501N, D506V(4-6)	K93A/F94A (7), F94A/K182Q/R184Q (7), V134M(5), A222G(8),(9), C229G(10), V252A/I267A(7), I339M(11), H400L(12) (13) (11),	F29/Q31(7), D26N/K27Q/F29A/Q31A and F29A/Q31A (7), L73A/L76A/F82A(7), G170V(11), V212A/L236A(7), Q232K(11), C237Y, R299W(9, 14, 15)	D26N/K27Q(7), Q232K/S250L(11), K249Q/Q259R/E270Q(7), V252A/I267A(7)	K51A/R62A(7), A222G(8),(9)

M120I (15) and G243D (8),(16),(15) are disease-associated mutations of surface residues that neither impair secretion nor reduce enzymatic activity. Either they are crucial for hitherto uncharacterized fI interactions, or the association with the disease is to be questioned.

R183S, A282T, R388H, K423R, R484L, E530Q, Y553S (6, 10, 17) are naturally occurring polymorphisms that map to surface regions of the protein, away from proposed cofactor and/or substrate interaction sites

W127X, E285K plus E287X, W468X, R456X, W528X (9, 10) (5, 6, 15, 18) premature stop codons give rise to truncated and therefore not functional forms of the protein.

Supporting Information References

1. Ullman CG & Perkins SJ (1997) The Factor I and follistatin domain families: the return of a prodigal son. *Biochem J* 326 (Pt 3):939-941.
2. Chamberlain D, Ullman CG, & Perkins SJ (1998) Possible arrangement of the five domains in human complement factor I as determined by a combination of X-ray and neutron scattering and homology modeling. *Biochemistry* 37(40):13918-13929.
3. Holm L & Rosenstrom P (2010) Dali server: conservation mapping in 3D. *Nucleic Acids Res* 38(Web Server issue):W545-549.
4. Geelen J*, et al.* (2007) A missense mutation in factor I (IF) predisposes to atypical haemolytic uraemic syndrome. *Pediatr Nephrol* 22(3):371-375.
5. Westra D*, et al.* (2010) Genetic disorders in complement (regulating) genes in patients with atypical haemolytic uraemic syndrome (aHUS). *Nephrol Dial Transplant* 25(7):2195-2202.
6. Fremeaux-Bacchi V*, et al.* (2004) Complement factor I: a susceptibility gene for atypical haemolytic uraemic syndrome. *J Med Genet* 41(6):e84.
7. Nilsson SC*, et al.* (2010) Analysis of binding sites on complement factor I that are required for its activity. *J Biol Chem* 285(9):6235-6245.
8. Servais A*, et al.* (2007) Primary glomerulonephritis with isolated C3 deposits: a new entity which shares common genetic risk factors with haemolytic uraemic syndrome. *J Med Genet* 44(3):193-199.
9. Caprioli J*, et al.* (2006) Genetics of HUS: the impact of MCP, CFH, and IF mutations on clinical presentation, response to treatment, and outcome. *Blood* 108(4):1267-1279.
10. Saunders RE*, et al.* (2007) The interactive Factor H-atypical hemolytic uremic syndrome mutation database and website: update and integration of membrane cofactor protein and Factor I mutations with structural models. *Hum Mutat* 28(3):222-234.
11. Nilsson SC*, et al.* (2009) Genetic, molecular and functional analyses of complement factor I deficiency. *Eur J Immunol* 39(1):310-323.
12. Vyse TJ*, et al.* (1996) The molecular basis of hereditary complement factor I deficiency. *J Clin Invest* 97(4):925-933.
13. Sadallah S, Gudat F, Laissue JA, Spath PJ, & Schifferli JA (1999) Glomerulonephritis in a patient with complement factor I deficiency. *Am J Kidney Dis* 33(6):1153-1157.
14. Nilsson SC*, et al.* (2010) Mutations in complement factor I as found in atypical hemolytic uremic syndrome lead to either altered secretion or altered function of factor I. *Eur J Immunol* 40(1):172-185.
15. Kavanagh D*, et al.* (2008) Characterization of mutations in complement factor I (CFI) associated with hemolytic uremic syndrome. *Mol Immunol* 45(1):95-105.
16. Nilsson SC*, et al.* (2007) A mutation in factor I that is associated with atypical hemolytic uremic syndrome does not affect the function of factor I in complement regulation. *Mol Immunol* 44(8):1835-1844.
17. Yuasa I*, et al.* (2008) Molecular basis of complement factor I (CFI) polymorphism: one of two polymorphic suballeles responsible for CFI A is Japanese-specific. *J Hum Genet* 53(11-12):1016-1021.
18. Kavanagh D*, et al.* (2005) Mutations in complement factor I predispose to development of atypical hemolytic uremic syndrome. *J Am Soc Nephrol* 16(7):2150-2155.